Journal of Materials Chemistry C

Accepted Manuscript

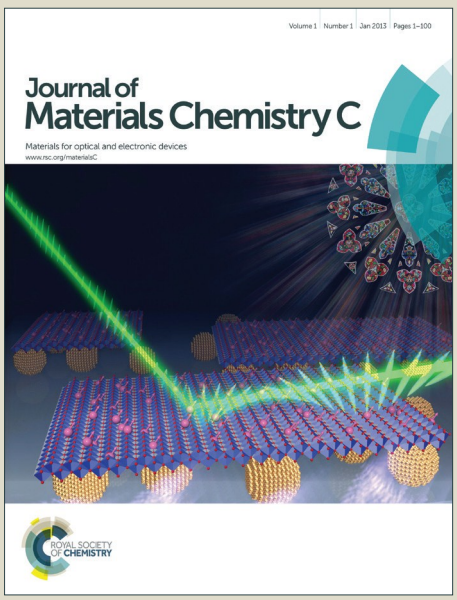

ROYAL SOCIETY OF CHEMISTRY

www.rsc.org/materialsC

Journal Name

ARTICLE

Thermoresponsive AIE polymers with fine-tuned response temperature

Received 00th January 20xx,
Accepted 00th January 20xx

DOI: 10.1039/x0xx00000x

www.rsc.org/

Tingzhong Li,[a] Sicong He,[c] Jianan Qu,[c] Hao Wu,[a] Shuizhu Wu,[a] Zujin Zhao,[a] Anjun Qin,[a] Rongrong Hu*[a] and Ben Zhong Tang*[ab]

A series of thermoresponsive AIE polymers were synthesized through the free radical copolymerization of thermosensitive *N*-isopropylacrylamide (NIPAM) monomer, regulative oligo(ethylene glycol) methacrylate (OEGMA) monomer or methyl methyacrylate (MMA) monomer, and fluorescent tetraphenylethene monomer. By adjusting the loading ratio of NIPAM and OEGMA/MMA, the hydrophilicity of the copolymers can be fine-tuned, which enables further modulation of the lower critical solution temperature (LCST) as well as the detection temperature range. Below the LCST, hydrogen bonds are formed between the polymer chain and water molecules, which lead to good solubility and weak emission of the polymers. Above the LCST, interchain or intrachain hydrogen bonds within polymers are favored to form emissive polymer aggregates.

Introduction

Fluorescent probes have attracted much attention, owing to their high sensitivity, fast response, easy accessibility, and non-invasive detection. Among them, thermoresponsive fluorescent probes with high temperature and spatial resolution in in-situ detections are highly desired.[1-2] They have been widely used in the study of hydrogen bonding systems,[3] protein folding and denaturation,[4-6] drug delivery,[7] etc.[8] Thermoresponsive polymers with lower critical solution temperature (LCST) are representative materials for temperature sensing and mapping, owing to their heating/cooling-driven reversible morphology transition in solution.[9] Materials such as organic compounds and polymers, molecular beacons, quantum dots, metal-doped nanomaterials and doped MOFs are developed as fluorescent thermometers.[10–13] Of all the widely studied thermoresponsive polymers such as poly(*N*-isopropyl acrylamide) (PNIPAM), poly(*N*-*n*-propyl acrylamide), poly(*N*,*N*-diethyl acrylamide), poly(*N*-ethyl acrylamide), poly(vinylcaprolactam), and oligo(ethylene glycol) methacrylate, PNIPAM shows drastic swelling transition at its LCST of 32 °C, attributed to the hydrophilic-lipophilic balance of the polymer.[14] In the fluorescent PNIPAMs, the temperature induced fluorescence variation are generally caused by thermal activation of nonradiative deactivation pathways. However, the nonradiative decay rate is generally enhanced with increasing temperature and thus leads to diminished luminescence intensity.[15]

Aggregation-induced emission (AIE) materials, in comparison to the traditional fluorophores with aggregation-caused quenching problem, are a promising type of "light-up" fluorescent probes.[16] AIE compounds are generally propeller-shaped compounds with no or weak luminescence in dilute solution, but they show enhanced fluorescence from single molecular state to aggregated state or after interaction with analytes.[17] AIE phenomenon was attributed to the restriction of intramolecular motions (RIM), including rotation and vibration.[18] In dilute solution, AIE molecules undergo active intramolecular motions which provide a non-radiative decay pathway of excited state; in the aggregated states when the molecules are close to each other, the intramolecular motions are restricted which block the non-radiative decay and induce emission. Owing to the high emission efficiency of the aggregated states, AIE materials have been extensively studied by a large number of research groups all over the world in organic light-emitting diodes, chemosensors, bioprobes and bioimaging.[19]

A few works have been reported to incorporate AIE structures into thermoresponsive polymers, which have demonstrated great advantages of such fluorescent temperature sensors. For example, a tetraphenylethene (TPE)-

[a] State Key Laboratory of Luminescent Materials and Devices, South China University of Technology, Guangzhou 510640, China.
[b] Department of Chemistry, The Hong Kong University of Science & Technology, Clear Water Bay, Kowloon, Hong Kong.
[c] Department of Electronic and Computer Engineering, The Hong Kong University of Science & Technology, Clear Water Bay, Kowloon, Hong Kong.

*Corresponding authors - msrrhu@scut.edu.cn

† Electronic Supplementary Information (ESI) available: Dye content-dependent fluorescence response, calibration curve of the absorbance versus dye content, ^{1}H NMR and IR spectra of the monomers and polymer examples, absorption spectra of P**1d** and P**2d**, temperature-dependent emission intensity of P**1a–f** and P**2a–d**, SEM image of the nanoparticles of P**1d**, fluorescence image of HeLa cells incubated

modified PNIPAM-based thermometer was reported with the fluorescence-response temperature range of 25–34 °C.[20] TPE was also incorporated into oligo(ethylene glycol)s to combine AIE properties and thermosensitivity in a class of compounds.[21-22] When heated above the phase-transition temperature, the compounds start to aggregate, which results in the restricted intramolecular rotation of TPE moieties as well as strong emission. A tetraphenylthiophene-functionalized PNIPAM was also reported to show complete emission quench when heated at temperatures above LCST.[23] Recently, a series of temperature sensitive TPE-containing PNIPAM/poly(methacrylic acid) interpenetrating polymer networks were reported to show fluorescence enhancement in the temperature range of 20.0–27.5 °C and stable fluorescence intensity region from 27.5-35.0 °C.[24] Some other works have also utilize AIE feature in thermoresponsive materials and the fluorescence was generally decreased by heating which show "light-off" behaviour.[25-27] However, few work has been reported focusing on the fine-tuning of the temperature sensitive range as well as the LCST of the polymer. In this work, a series of tunable thermoresponsive copolymers was prepared from thermosensitive *N*-isopropyl acrylamide (NIPAM) monomer, regulative oligo(ethylene glycol) methacrylate (OEGMA, M_n = 500) or methyl methacrylate (MMA) monomer, and fluorescent TPE monomer through free radical polymerization. By adjusting the hydrophilicity of the copolymer, LCST as well as the detection temperature range can be precisely controlled towards the physiological temperature.

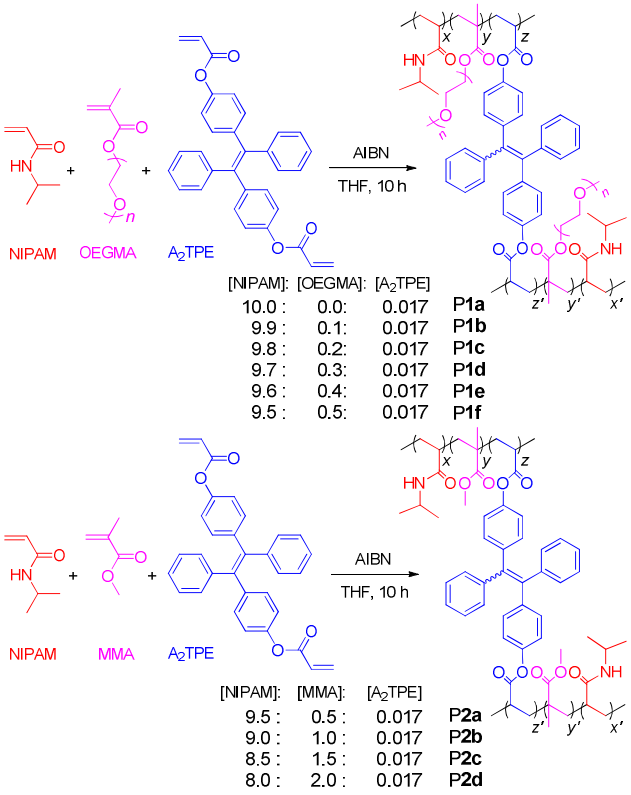

Scheme 1. Synthetic routes of thermoresponsive AIE polymers.

Results and Discussion

Synthesis and characterizations

The synthetic routes of thermoresponsive AIE polymers are shown in Scheme 1. TPE-containing monomer A_2TPE was prepared through McMurry coupling reaction and the following esterification according to our previous reported work,[28] which was copolymerized with NIPAM to afford temperature sensitive polymers. Furthermore, more hydrophilic OEGMA or less hydrophilic MMA compared with NIPAM was incorporated into the polymers as a third component, respectively, to fine-tune the hydrophilicity of the resultant polymers. The AIBN-initiated free radical copolymerizations of the three components can afford water soluble polymers P**1–2** in high yields and good reproducibility.

In such a hydrophilic copolymer, trace amount of the hydrophobic TPE moieties embedded in the polymer backbone shows great influence to its temperature-fluorescence response. The loading ratio of A_2TPE was hence optimized first (Figure S1). When it was tuned from 0.17–0.33 mol% in the copolymerization of NIPAM, OEGMA, and A_2TPE, the PL spectra of aqueous solutions of each resultant polymer were measured at 42 and 20 °C, respectively. The fluorescence contrast of the polymer at 42 and 20 °C is large when the feeding ratio of A_2TPE is 0.17 mol%, suggesting the optimal fluorescence sensitivity, water solubility, and phase transition behaviour at varied temperatures. Two series of copolymers P**1a–f** and P**2a–d** were then prepared with the fixed feeding ratio of A_2TPE of 0.17 mol%, and varied feeding ratio of NIPAM and OEGMA, or NIPAM and MMA, respectively (Table 1). Generally, copolymers with good yield and high M_w about 20 000 were obtained.

UV-vis and ^{1}H NMR spectra of each copolymer were used to characterize the structure and the ratio of the three components. UV absorption spectra were used to quantify the amount of the fluorophores existed in each polymer. A calibration absorption-concentration curve was first established using A_2TPE as a standard compound (Figure S2). The absorption spectra of THF solutions of the polymers with identical concentration were then measured. The absorbance of the polymers all fell into the calibration curve, which could reveal the exact fluorophore concentrations in each polymer as calculated in Table 1. Furthermore, from the ^{1}H NMR spectra of the monomers and polymers shown in Figure S3 as the example, the absorption peaks for the acrylate vinyl protons all disappeared, while the CH proton from NIPAM emerged in the polymer spectra, suggesting the expected structure. From the integration ratio of the peaks at 3.83 ppm, and 3.23, or 3.55 ppm, the molar ratio of NIPAM and OEGMA or MMA can be calculated, respectively, which is in accordance with the feeding ratio of the three monomers (Table 1).

Contact angle measurement

Through the subtle structural variation, the hydrophilicity of the polymers can be modulated, which was characterized by the contact angle measurement of their thin films (Figure 1). The polymers have more hydrophilic surfaces compared with

Table 1. Properties of the Copolymers Prepared by Free Radical Polymerization

Entry		molar ratio[a]	yield (%)	M_w[b]	PDI	molar ratio[c]
		[NIPAM]: [OEGMA]: [A_2TPE]				[NIPAM]: [OEGMA]: [A_2TPE]
1	P**1a**	10.0 : 0.0 : 0.017	90	18 500	1.50	10.0 : 0.0 : 0.013
2	P**1b**	9.9 : 0.1 : 0.017	80	19 400	1.49	9.9 : 0.1 : 0.018
3	P**1c**	9.8 : 0.2 : 0.017	80	19 800	1.55	9.8 : 0.2 : 0.017
4	P**1d**	9.7 : 0.3 : 0.017	85	21 000	1.31	9.7 : 0.3 : 0.012
5	P**1e**	9.6 : 0.4 : 0.017	78	21 900	1.43	9.6 : 0.4 : 0.013
6	P**1f**	9.5 : 0.5 : 0.017	77	21 900	1.49	9.2 : 0.8 : 0.014
		[NIPAM]: [MMA]: [A_2TPE]				[NIPAM]: [MMA]: [A_2TPE]
7	P**2a**	9.5 : 0.5 : 0.017	95	18 900	1.49	9.3 : 0.7 : 0.008
8	P**2b**	9.0 : 1.0 : 0.017	95	19 100	1.69	9.0 : 1.0 : 0.011
9	P**2c**	8.5 : 1.5 : 0.017	92	21 800	1.71	8.6 : 1.4 : 0.013
10	P**2d**	8.0 : 2.0 : 0.017	97	24 500	1.68	8.0 : 2.0 : 0.015

[a]The feeding ratio of NIPAM, OEGMA (or MMA) and A_2TPE. [b]M_w and PDI are determined by GPC. [c]Ratio of NIPAM and OEGMA (or MMA) was calculated from the integration ratios of ^{1}H NMR peaks at δ = 3.83 and δ = 3.23 (or δ = 3.55). Ratio of A_2TPE was calculated from UV absorption spectra at 310 nm.

the glass and P**1a–f** with OEGMA moieties are more hydrophilic compared with P**2a–d** with MMA moieties. When the ratio of MMA increases, the contact angle increases with increased hydrophobicity; when the ratio of OEGMA increases, the contact angle decreases with increased hydrophilicity. Furthermore, take P**1d** for example, the contact angle of the polymer thin film at room temperature is 12°, representing a very hydrophilic surface. When the thin film was heated to 50 °C, the contact angle increased to 38°, indicating a polymer conformation transition at different temperatures.

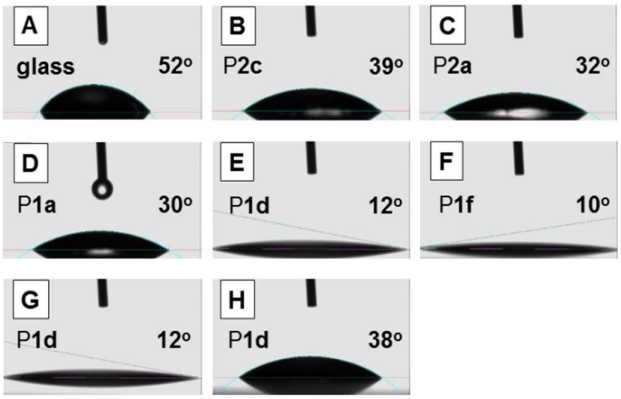

Figure 1. Photographs of contact angles of (A) glass, (B) P**2c**, (C) P**2a**, (D) P**1a**, (E) P**1d**, (F) P**1f**. Thin film of P**1d** at (G) room temperature and (H) 50 °C, respectively.

Temperature-dependent transmittance

The temperature-dependent transmittance of the copolymers was then studied to measure the LCST which was the temperature with 90% transmittance of the original solution (Figure 2A).[29] In the dilute aqueous solutions at room temperature, all the polymers are transparent with P**1d** as the example shown in Figure 3. When the solution was gradually heated up to 50 °C, the polymer turned to be turbid. Such change in solution transmittance can be reversibly repeated. In the transmittance spectra of the polymers, a sharp drop was observed above a threshold temperature. The polymers with subtle structural difference showed different temperature-dependent transmittance. The LCSTs of the polymers are summarized in Figure 2B. From P**1a**–**1f** with increasing amount of OEGMA in the polymer structure from 0 to 5 mol%, the LCST gradually increased from 31 °C to 37 °C, representing a linear relationship of the LCST with the amount of OEGMA. It can be estimated that each increase of 1 mol% of OEGMA may result in 1.33 °C increase in LCST. Similarly in P**2a**–**2d** with increasing MMA amount from 5 to 20 mol%, the LCST gradually decreased.

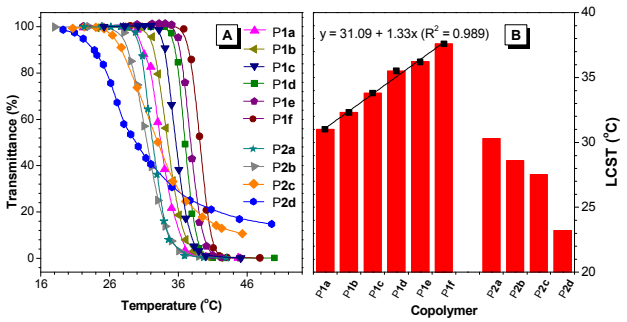

Figure 2. (A) Temperature-dependent transmittance of aqueous solutions of P**1a–f** and P**2a–d** at 650 nm. (B) LCST of P**1a–f** and P**2a–d**. Concentration: 3 mg/mL.

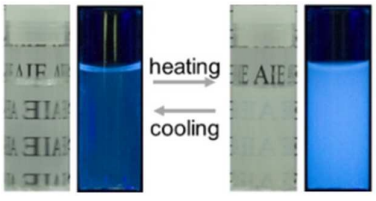

Figure 3. Photographs of aqueous solution of P**1d** upon heating and cooling taken under daylight (left) and UV irradiation (right). Concentration: 1 mg/mL.

Aggregation-induced emission

The photophysical properties of the polymers were then investigated. The UV absorption spectra of P**1d** and P**2d** were first studied as examples in aqueous solutions (Fig. S5). The absorption maxima of both polymers were located at about 310 nm, corresponding to the absorption maximum of the A_2TPE units. The emission spectra of P**1d** in THF/hexane mixtures with different hexane fractions were then investigated as shown in Figure 4. The dilute THF solution of P**1d** emits almost no light upon photoexcitation, because the A_2TPE fluorophores can undergo intramolecular rotations in solution which consume excited state energy non-radiatively. With less than 50 vol% hexane, a poor solvent of the polymer, was added into the solvent system, the emission is still weak. The emission intensity gradually increases afterwards and reached about 20 fold of that in pure THF solution when 90 vol% hexane was added. In such medium, the polymer aggregated and the intramolecular motions of the A_2TPE units were restricted by the steric constraint which boosted the emission, demonstrating typical aggregation-induced emission characteristics. Other polymers also possess similar AIE feature.

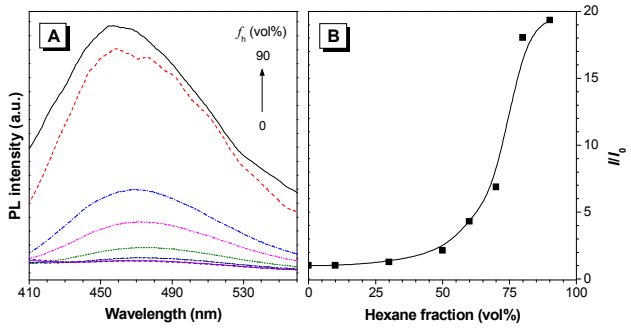

Figure 4. (A) Emission spectra of P**1d** in THF/hexane mixtures with different hexane contents, (B) plots of emission intensity of P**1d** versus the volume fraction of hexane at 478 nm. *I* is the emission intensity of P**1d** in THF/hexane mixtures with different hexane content. I_0 is the emission intensity of P**1d** in THF solution. Concentration: 1 mg/mL. Excitation wavelength: 310 nm.

Temperature-dependent fluorescence

The fluorescence of the AIE polymers is dependent on the polymer conformation, which can be tuned by temperature in the cases of thermoresponsive polymers. The temperature-dependent fluorescence of the polymers was then investigated using P**1d** as an example (Figure 5A). The aqueous solution of P**1d** was slowly heated from 32 °C to 50 °C and the PL spectra were recorded. The emission peak at about 480 nm was gradually enhanced with increasing temperature. The temperature-dependent fluorescence enhancement of P**1d** was summarized in Figure 5B, demonstrating a linear relationship between the temperature range of 36–42 °C. It is worth noticing that there is a small peak at about 30 °C before the LCST of the polymer, suggesting that such fluorescence response can provide higher sensitivity with more details on the temperature-dependent variations of polymer conformation, which can hardly be achieved by other methods.

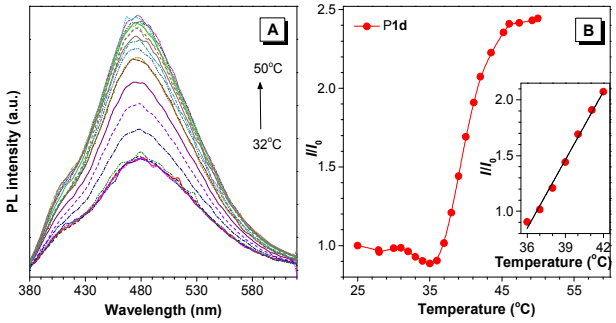

Figure 5. (A) Temperature-dependent emission spectra of aqueous solution of P**1d** from 32 to 50 °C. (B) Emission intensity of P**1d** at 478 nm versus the temperature. Inset: the plot of linear fitting of I/I_0 of P**1d** from 36 to 42 °C. *I* is the emission intensity at different temperature. I_0 is the emission intensity at 32 °C. Concentration: 0.02 mg/mL. Excitation wavelength: 310 nm.

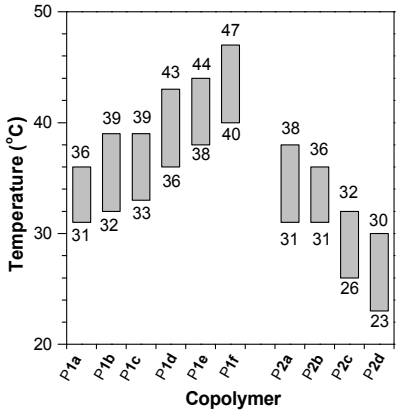

Figure 6. Linear response temperature range of the aqueous solutions of P**1a–f** and P**2a–d**. Concentration: 0.02 mg/mL. Excitation wavelength: 310 nm.

Similar phenomenon was observed for other polymers and their temperature-dependent emission enhancements were shown in Figure S6. The emission intensities of all polymers were raised dramatically after a threshold temperature. The temperature-sensitive ranges of P**1a–f** and P**2a–d**, covering from 23 °C to 47 °C, were summarized in Figure 6, demonstrating the precise modulation and continuously fine-tuned temperature-sensitive range within the biologically important temperature range. P**1a–f** generally response at higher temperatures compared with P**2a–d** and the average linear responsive temperature range is about 6 °C. For P**1a–f**, with increasing amount of OEGMA and hydrophilicity, the polymer generally starts to respond at a higher temperature. Similar for P**2a–d**, with increasing amount of MMA and hydrophobicity, the polymer starts to respond at lower temperatures. In general, the threshold temperature in the temperature-dependent PL enhancement spectra is consistent with the LCST of each polymer determined by transmittance.

Moreover, as can be seen from Figure 5B and Figure S6, unlike the reported temperature-sensitive fluorescent polymers, the AIE polymers can provide more details in the early stage of the morphology change. Most of the copolymers possess a fluctuation below LCST, indicating the multiple influences of temperature on the fluorescence. For example, the thermally activated molecular motion may quench the emission, while the intermolecular and intramolecular hydrogen bonding is favored at different temperatures, which may cause reduced or enhanced emission, respectively.

The repeatability and reversibility of the heating-cooling cycle were investigated by alternatively heating the aqueous solution of P**1d** to 50 °C and cooling it to 27 °C (Figure 7A). The fluorescence intensities were recorded at 43 °C and 33 °C for each cycle as shown in Figure 7B, suggesting good consistency.

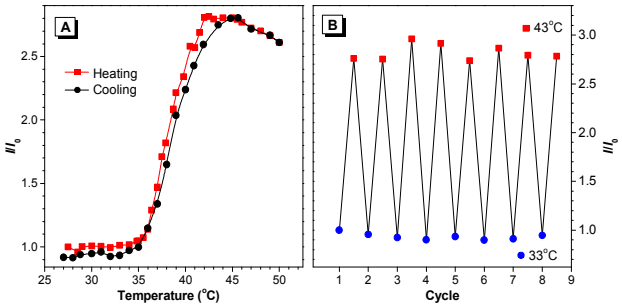

Figure 7. (A) Temperature-dependent fluorescence of aqueous solution of P**1d** in a heating-cooling cycle. (B) Fluorescence intensities at 478 nm recorded at 43 °C and 33 °C at each heating-cooling cycle. I is the emission intensity at different temperature. I_0 is the emission intensity at 27 °C. Concentration: 0.05 mg/mL. Excitation wavelength: 310 nm.

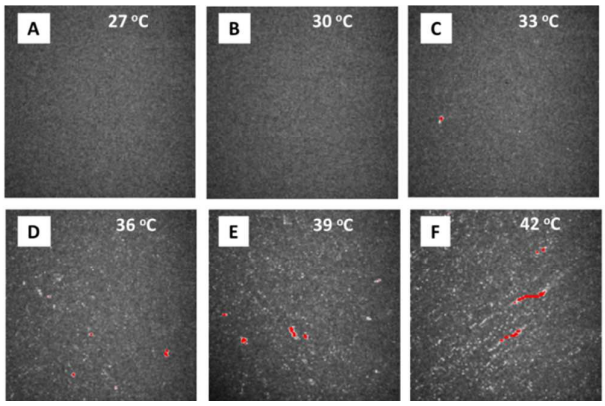

Figure 8. Image of time-resolved two-photon excitation fluorescence of aqueous solution of P**1d** at (A) 27 °C, (B) 30 °C, (C) 33 °C, (D) 36 °C, (E) 39 °C, and (F) 42 °C. The field of view is 100 μm × 100 μm. Resolution is 128 × 128 pixels. Concentration: 1 mg/mL. Excitation wavelength: 720 nm.

Fluorescence lifetime imaging and cell imaging

Of all the temperature-dependent fluorescence parameters, fluorescence lifetime is independent of the concentration, size or geometry of molecules. It also was not affected by light scattering, reflection or the intensity fluctuation of the excitation source.[30] The fluorescence lifetime images of the aqueous solution of P**1d** at different temperatures were hence recorded as shown in Figure 8. The intensity of each pixel in the images is proportional to the exact photon counts and the pixels in red represent the aggregated polymers with saturated intensity, or photon counts more than 200. The fluorescence lifetime and aggregated area both show dependence on the temperature (Figure 8 and Figure S7).

The water-soluble thermoresponsive AIE polymers were then investigated in cell imaging. For example, HeLa cells were incubated with P**2c** for 1.5 h. The fluorescence image was shown in Figure S9, which proved the biocompatibility and cell permeability of the polymers.

Variable-temperature ^{1}H NMR

^{1}H NMR of P**1d** was then conducted at varied temperatures to elucidate the molecular morphology change of the polymer (Figure 9). As can be seen, all aliphatic protons in NIPAM moiety, OEGMA moieties, as well as the polymer backbone, are continuously shifted to lower field upon heating from 26 °C to 50 °C. For example, the methyl groups in NIPAM units have shifted from 1.21 ppm to 1.43 ppm, demonstrating a shielding effect at high temperature. The polymer chains shrink and form compact particles at high temperature, which provide a more crowded environment for the protons and the shielding effect hence took place to move the ^{1}H NMR peaks toward lower field.

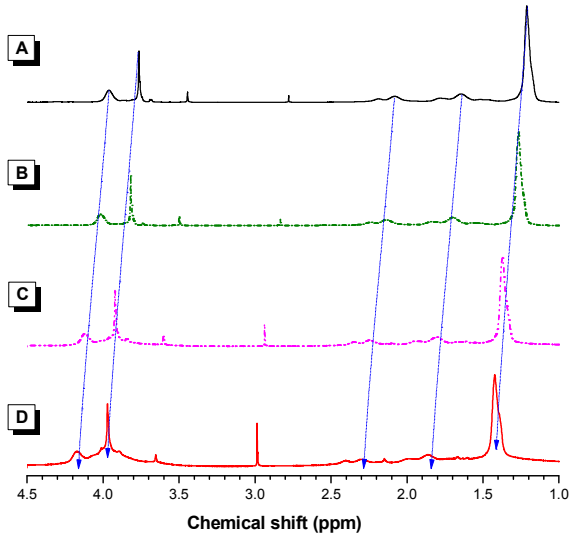

Figure 9. ^{1}H NMR spectra of P**1d** at (A) 26 °C, (B) 35 °C, (C) 45 °C, and (D) 50 °C in D_2O.

Below LCST, the amide groups of the polymers can form hydrogen bonds with water molecules and the polymers are well-dissolved with stretched molecular conformation in the aqueous solutions. The TPE moieties lie in a flexible environment and can undergo intramolecular rotation to consume the excited state energy, which results in low

fluorescence intensity. Above LCST, the intermolecular hydrogen bonding with solvent molecules is replaced by the intrachain hydrogen bonding which is favored at such temperature. The polymer molecules shrink to form compact nanoparticles instead of swelling coils, evidenced by the SEM microscopic image of the nanoparticles of P**1d** with diameters ranging from 100 to 200 nm formed in the aqueous solution at 50 ^{o}C (Figure S8). Meanwhile, hydrophilic parts of the polymer have formed intramolecular hydrogen bond and hold the polymer chains closely, which left the hydrophobic parts of the polymer expose to the environment. In another word, heating reduces the hydrophilicity of the polymer surface. In the compact polymer nanoparticles, the TPE moieties are rigidified and the intramolecular rotations are restricted, rendering the polymer emissive. When the polymer solution is further cooled below LCST, the intermolecular hydrogen bonds of the polymer with water molecules are recovered and become dominant again, completing a reversible cycle.

Conclusions

In this work, water-soluble thermoresponsive AIE copolymers with fine-tuned LCST and response temperature were synthesized by free radical polymerization of NIPAM, OEGMA or MMA, and A_2TPE monomers. By adjusting the hydrophilicity of the copolymers, LCST as well as the detection temperature range can be precisely controlled towards the physiological temperature. AIE moieties are weakly emissive in aqueous solutions when the copolymers are well-dissolved at low temperature, but emit intensely when the copolymers shrink as particles at temperature above LCST. These water-soluble thermoresponsive AIE copolymers are promising in a series of biological studies such as cell imaging.

Experimental Section

Materials. *N*-Isopropyl acrylamide (NIPAM), 4-hydroxybenzophenone, benzophenone, and acryloyl chloride were obtained from TCI. Oligo (ethylene glycol) methacrylate (OEGMA, M_n = 500 g/mol) was purchased from Aldrich. 2, 2'-azobisisobutyronitrile (AIBN) and methyl methyacrylate (MMA) were received from Damao Chemical Reagent Factory. A_2TPE was prepared according to our published work.[28] NIPAM, AIBN, and A_2TPE were recrystallized prior to use. Tetrahydrofuran was distilled with sodium and benzophenone under nitrogen immediately prior to use. All other commercially available reactants and reagents were used as received without further purification.

Instruments. FT-IR spectra were recorded on a Brucker Vector 33 FT-IR spectrometer using KBr as carrier. ^{1}H NMR spectra were measured on a Brucker Avance 600MHz NMR spectrometer using deuterium oxide or deuterated dimethylsulfoxide as solvent. UV-vis spectra were recorded on a Shimadzu UV-2600 spectrometer. Temperature-dependent transmittance was determined by monitoring the optical transmittance at 650 nm on Shimadzu UV2600 spectrophotometer with a thermal controller. Number (M_n) and weight-average (M_w) molecular weights and polydispersity indices (PDI = M_w/M_n) of the copolymers were estimated by a Waters Associates 515 gel permeation chromatography (GPC) system. THF was used as eluent at a flow rate of 1 mL/min. A set of monodispersed linear polystyrenes covering the M_w range of 10^3-10^7 g/mol were utilized as standards for molecular weight calibration. Photoluminescence (PL) spectra were measured on a Perkin-Elmer LS 55 spectrofluorometer with a thermal controller. Temperature-dependent PL spectra were recorded by monitoring the PL intensities at 478 nm at different temperatures. SEM image was taken on a SEM instrument (Merlin ZEISS) at an accelerating voltage of 5 kV. Water contact angles were measured on a contact angle meter (OCA 40 Micro). Contact Angles were read after liquid drop extending on the substrate for 10 s. Time-resolved fluorescence imaging was recorded on a home-built instrument equipped with a time-correlated single photon counting module and the sample was excited with two-photon excitation wavelength at 720 nm at different temperatures. Data was analyzed by setting a threshold value to extract the polymer aggregates in the fluorescence images, applying the bi-exponential fitting of the fluorescence lifetime of the extracted pixels, and calculating the areas of the polymer aggregates.

Acknowledgements

This work was partially supported by the National Science Foundation of China (21404041, 21490573, 21490574), the National Basic Research Program of China (973 Program; 2013CB834701), the Fundamental Research Funds for the Central Universities, and the Research Grants Council of HongKong (16305014, 604913, 602212, and 604711). B.Z.T. thanksthe support of the Guangdong Innovative Research TeamProgram (201101C0105067115).

Notes and references

1 K. Okabe, N. Inada, C. Gota, Y. Harada, T. Funatsu and S. Uchiyama, *Nat. Commun.*, 2012, **3**, 705.
2 C. Chen and C. Chen, *Chem. Commun*, 2011, **47**, 994.
3 L. B. Sagle, Y. Zhang, V. A. Litosh, X. Chen, Y. Cho and P. S. Cremer, *J. Am. Chem. Soc.*, 2009, **131**, 9304.
4 B. S. Gupta, M. Taha and M. Lee, *Phys. Chem. Chem. Phys.*, 2015, **17**, 1114.
5 J. Heyda and J. Dzubiella, *J. Phys. Chem. B*, 2014, **118**, 10979.
6 D. Mukherji, C. M. Marques and K. Kremer, *Nat. Commun.*, 2014, **5**. 4882.
7 A. Bajpai, S. K. Shukla, S. Bhanu and S. Kankane, *Prog. Polym. Sci.* 2008, **33**, 1088.
8 G. Graziano, *Int. J. Biol. Macromol.*, 2000, **27**, 89.
9 C. Pietsch, R. Hoogenboom and U. S. Schubert, *Polym. Chem.*, 2010, **1**, 1005.
10 Y. Cui, H. Xu, Y. Yue, Z. Guo, J. Yu, Z. Chen, J. Gao, Y. Yang, G. Qian and B. Chen, *J. Am. Chem. Soc.*, 2012, **134**, 3979.
11 R. F. D'Vries, S. Alvarez-Garcia, N. Snejko, L. E. Bausa, E. Gutierrez-Puebla, A. de Andres and M. Angeles Monge, *J. Mater. Chem. C*, 2013, **1**, 6316.

12 G. Ke, C. Wang, Y. Ge, N. Zheng, Z. Zhu and C. J. Yang, *J. Am. Chem. Soc.*, 2012, **134**, 18908.
13 L. M. Maestro, C. Jacinto, U. R. Silva, F. Vetrone, J. A. Capobianco, D. Jaque and J. Garcia Sole, *Small*, 2011, **7**, 1774.
14 K. N. Plunkett, X. Zhu, J. S. Moore and D. E. Leckband, *Langmuir*, 2006, **22**, 4259.
15 Y. Cui, F. Zhu, B. Chen and G. Qian, *Chem. Commun.*, 2015, **51**, 7420.
16 J. Luo, Z. Xie, J. W. Y. Lam, L. Cheng, H. Chen, C. Qiu, H. S. Kwok, X. Zhan, Y. Liu, D. Zhu and B. Z. Tang, *Chem. Commun.*, 2001, 1740.
17 Y. Hong, J. W. Y. Lam and B. Z. Tang, *Chem. Commun.*, 2009, 4332.
18 J. Mei, Y. Hong, J. W. Y. Lam, A. Qin, Y. Tang and B. Z. Tang, *Adv. Mater.*, 2014, **26**, 5429.
19 R. Hu, N. L. C. Leung and B. Z. Tang, *Chem. Soc. Rev.*, 2014, **43**, 4494.
20 L. Tang, J. K. Jin, A. Qin, W. Zhang Yuan, Y. Mao, J. Mei, J. Zhi Sun and B. Z. Tang, *Chem. Commun.*, 2009, 4974.
21 Y. Chen, J. W. Y. Lam, S. Chen and B. Z. Tang, *J. Mater. Chem. C*, 2014, **2**, 6192.
22 X. Yin, F. Meng and L. Wang, *J. Mater. Chem. C*, 2013, **1**, 6767.
23 C. Lai, R. Chien, S. Kuo and J. Hong, *Macromolecules*, 2011, **44**, 6546.
24 H. Zhou, F. Liu, X. Wang, H. Yan, J. Song, Q. Ye, B. Z. Tang and J. Xu, *J. Mater. Chem. C*, 2015, **3**, 5490.
25 Y. Jiang, X. Yang, C. Ma, C. Wang, Y. Chen, F. Dong, B. Yang, K. Yu and Q. Lin, *ACS Appl. Mater. Inter.*, 2014, **6**, 4650.
26 X. Yang, Y. Jiang, B. Shen, Y. Chen, F. Dong, K. Yu, B. Yang and Q. Lin, *Polym. Chem*., 2013, **4**, 5591.
27 Y. Niu, F. Zhang, Z. Bai, Y. Dong, J. Yang, R. Liu, B. Zou, J. Li and H. Zhong, *Adv. Opt. Mater*., 2015, **3**, 112-119.
28 R. Hu, J. W. Y. Lam, Y. Yu, H. H. Y. Sung, L. D. Williams, M. M. F. Yuen and B. Z. Tang, *Polym. Chem.*, 2013, **4**, 95.
29 X. Liu, F. Cheng, H. Liu and Y. Chen, *Soft Matter*, 2008, **4**, 1991.
30 K. Okabe, N. Inada, C. Gota, Y. Harada, T. Funatsu and S. Uchiyama, *Nat. Commun*. 2012, **3**, 705.

Thermoresponsive AIE polymer with fine-tuned response temperature

Tingzhong Li, Sicong He, Jianan Qu, Zujin Zhao, Anjun Qin, Rongrong Hu and Ben Zhong Tang

Graphical abstract

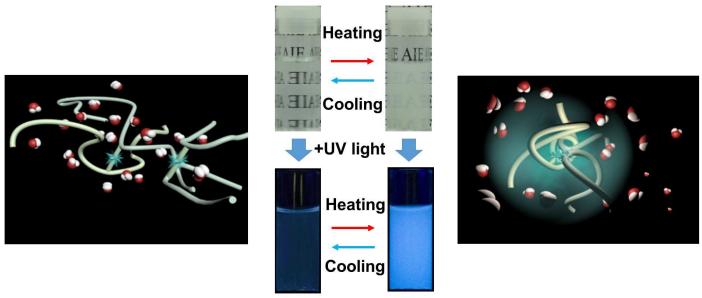

A series of thermoresponsive aggregation-induced emission polymers with fine-tuned hydrophilicity are synthesized as fluorescent thermometers with tunable response temperature.